Solution Structure of an Oligodeoxynucleotide Containing the Malondialdehyde Deoxyguanosine Adduct N^2-(3-Oxo-1-propenyl)-dG (Ring-Opened M_1G) Positioned in a $(CpG)_3$ Frameshift Hotspot of the *Salmonella typhimurium hisD3052* Gene†

Hui Mao,‡,§ G. Ramachandra Reddy,||,⊥ Lawrence J. Marnett,|| and Michael P. Stone*,‡

Departments of Chemistry and Biochemistry, Center in Molecular Toxicology, A. B. Hancock, Jr., Memorial Laboratory for Cancer Research, Vanderbilt University, Nashville, Tennessee 37235

Received May 4, 1999; Revised Manuscript Received August 5, 1999

ABSTRACT: The refined solution structure for the ring-opened N^2-(3-oxo-1-propenyl)-dG derivative of the malondialdehyde deoxyguanosine adduct M_1G [3-(2′-deoxy-β-D-*erythro*-pentofuranosyl)pyrimido[1,2-*a*]-purin-10(3*H*)-one] in d(ATCGCXCGGCATG)·d(CATGCCGCGCGAT) [X being N^2-(3-oxo-1-propenyl)-dG], containing the $d(CpG)_3$ frameshift hotspot of the *Salmonella typhimurium hisD3052* gene, is presented. When inserted into this duplex, M_1G underwent spontaneous ring opening to N^2-(3-oxo-1-propenyl)-dG. NMR analysis revealed that N^2-(3-oxo-1-propenyl)-dG induced minor structural perturbations in the *hisD3052* oligodeoxynucleotide. However, the stability of the duplex DNA was reduced; the N^2-(3-oxo-1-propenyl)-dG-modified *hisD3052* oligodeoxynucleotide exhibited a 14 °C decrease in T_m relative to that of the native oligodeoxynucleotide. The modified guanine maintained stacking interactions with neighboring bases but was not Watson−Crick hydrogen bonded. A total of 13 NOEs were observed from the 3-oxo-1-propenyl moiety protons of N^2-(3-oxo-1-propenyl)-dG to DNA protons. Molecular dynamics calculations, restrained by 602 distance restraints derived from experimental NOE measurements and 23 empirical distance restraints, converged with pairwise rmsd differences of <0.90 Å. The sixth-root residual factor with the NMR data was 9.1×10^{-2}. The cytosine complementary to N^2-(3-oxo-1-propenyl)-dG was pushed toward the major groove but maintained partial stacking interactions with its neighboring bases. The modified guanine remained in the anti conformation, while the 3-oxo-1-propenyl moiety was positioned in the minor groove of the duplex. Possible correlations between the relatively small structural perturbations induced in this DNA duplex by N^2-(3-oxo-1-propenyl)-dG and the mutagenic spectrum of M_1G are discussed.

Endogenous mutagens represent a class of molecules to which humans are continuously exposed at low levels and are thus implicated as causal factors in human cancer. Malondialdehyde (MDA)[1] is a toxic and mutagenic metabolite produced by lipid peroxidation (*1*) and prostaglandin biosynthesis (*2*, *3*). MDA is mutagenic in bacterial (*4*, *5*) and mammalian cells (*6*) and is carcinogenic in rats (*7*). MDA reacts with DNA (*8*−*13*). At physiological pH, the major adduct is a pyrimidopurinone formed by reaction with guanine [M_1G, 3-(2′-deoxy-β-D-*erythro*-pentofuranosyl)pyrimido[1,2-*a*]purin-10(3*H*)-one] (*8*, *9*, *14*−*16*). M_1G has been identified in DNA from rodent (*17*) and human (*18*, *19*) tissue samples, as have other exocyclic purine lesions (*20*−*22*), suggesting their formation in vivo. The M_1G adduct has been quantitated by mass spectral (*18*, *23*), postlabeling (*24*, *25*), and immunochemical (*26*) techniques. It represents the most abundant exocyclic DNA adduct present endogenously in human DNA (*13*, *23*−*25*). Site-specific mutagenesis experiments indicate it is an efficient premutagenic lesion (*27*). Thus, M_1G is a likely mediator of human genetic disease.

M_1G is stable at physiological pH but undergoes rearrangement to the ring-opened derivative N^2-(3-oxo-1-propenyl)-dG under basic conditions (Scheme 1). Remarkably, when inserted into duplex DNA opposite cytosine at neutral pH, M_1G spontaneously and quantitatively converts to N^2-(3-oxo-1-propenyl)-dG (*28*). Ring opening is reversible upon thermal denaturation of the duplex. The exocyclic amino group of the complementary cytosine promotes ring-opening of M_1G, probably by attack at C8 of the 1,N^2-exocyclic ring.

† This research was supported by NIH Grants CA-55678 (M.P.S.) and CA-47479 (L.J.M.). The NMR spectrometer was supported in part by NIH Shared Instrumentation Program RR-05805, and the Vanderbilt Center in Molecular Toxicology, ES-00267. This study made use of the National Magnetic Resonance Facility at Madison (NMRFAM). NMRFAM equipment was funded by the University of Wisconsin, NSF Grants DMB-8415048 and BIR-9214394, NIH Grants RR-02301, RR-02781, and RR08438, and the USDA. This study used the Atlanta High Field NMR Facility at Georgia State University, funded by the State of Georgia and NSF Grant BIR-9214443.

* To whom correspondence should be addressed. Phone: (615) 322-2589. Fax: (615) 343-1234. E-mail: stone@toxicology.mc.vanderbilt.edu.

‡ Department of Chemistry, Center in Molecular Toxicology, A. B. Hancock, Jr., Memorial Laboratory for Cancer Research, Vanderbilt University.

§ Present address: Frederik Philips Magnetic Resonance Research Center, Department of Radiology, Emory University School of Medicine, 1364 Clifton Rd. NE, Atlanta, GA 30322.

|| Department of Biochemistry, Center in Molecular Toxicology, A. B. Hancock, Jr., Memorial Laboratory for Cancer Research, Vanderbilt University.

⊥ Present address: Lumigen Inc., 24485 W. 10 Mile Rd., Southfield, MI 48034.

10.1021/bi9910124 CCC: $18.00
Published on Web 09/24/1999

Scheme 1: (A) Formation of M_1G via [1,2-*a*] Cyclization of Deoxyguanosine by β-Hydroxyacrolein, (B) Ring Opening of the M_1G Lesion to N^2-(3-Oxo-1-propenyl)-dG, and (C) Amino−Enol Tautomerization of N^2-(3-Oxo-1-propenyl)-dG

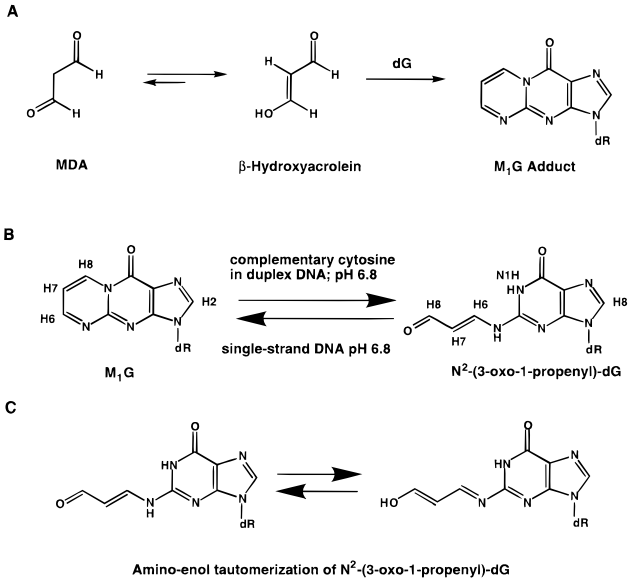

Thus, the DNA duplex plays an active role in directing the metabolism of MDA by catalyzing the chemical transformation of M_1G to N^2-(3-oxo-1-propenyl)-dG. The substantial structural difference between M_1G and N^2-(3-oxo-1-propenyl)-dG suggests that the two forms of this adduct might be processed differently in vivo, and that the disposition of the M_1G adduct in vivo may be dependent upon the ratio of ring-closed to ring-opened M_1G during replication or repair. Accordingly, it was of interest to examine the solution structure of the ring-opened N^2-(3-oxo-1-propenyl)-dG lesion in duplex DNA.

In the work presented here, M_1G was introduced into d(ATCGCXCGGCATG) (X being M_1G), derived from the *Salmonella typhimurium hisD3052* gene, a hotspot for frameshift mutations, and an oligodeoxynucleotide duplex in which we had previously examined the 1,N^2-propanodeoxyguanosine (PdG) adduct, a structural model for M_1G (*29*−*31*) (Scheme 2). When annealed with the complementary strand d(CATGCCGCGCGAT) containing cytosine

Scheme 2: Sequence and Numbering of the *S. typhimurium hisD3052* Oligodeoxynucleotide

5′-A^{-2}T^{-1}C^{1} G^{2} C^{3} X^{4} C^{5} G^{6} G^{7} C^{8} A^{9} T^{10}G^{11}-3′
3′-T^{24}A^{23}G^{22}C^{21}G^{20}C^{19}G^{18}C^{17}C^{16}G^{15}T^{14}A^{13}C^{12}-5′

opposite the M_1G adduct, spontaneous opening of the exocyclic ring of M_1G to N^2-(3-oxo-1-propenyl)-dG occurred. The solution structure of this N^2-(3-oxo-1-propenyl)-dG adducted oligodeoxynucleotide, obtained from molecular dynamics calculations using distance restraints derived from NMR (*32*), revealed that N^2-(3-oxo-1-propenyl)-dG stacked with both the 5′- and 3′-neighbor base pairs. The adducted duplex retained a B-DNA-like conformation without long-range structural perturbations, but with modest localized changes at the adducted site and neighboring base pairs. The complementary cytosine protruded slightly into the major groove of DNA. The ring-opened M_1G·C base pair was found in the anti conformation.

MATERIALS AND METHODS

Materials. The synthesis of base-sensitive M_1G-adducted oligodeoxynucleotides required base protection using the 2-(acetoxymethyl)benzoyl (AMB) group, which was readily removed using anhydrous potassium carbonate/methanol (*33*). The M_1G-modified oligodeoxynucleotide was deprotected and purified by reverse phase and anion exchange HPLC. The sample was maintained between pH 6 and 7 during purification. The adducted oligodeoxynucleotide was desalted using gel filtration (BioGel P-2). Its purity was verified by ^{32}P-end labeling followed by denaturing polyacrylamide gel electrophoresis. Unmodified oligodeoxynucleotides were purchased from the Midland Certified Reagent Co. (Midland, TX). They were purified by reverse phase and anion exchange HPLC. The sample purity was checked using a SureCheck oligodeoxynucleotide analysis kit (Amersham Pharmacia).

NMR Sample Preparation. The concentrations of the oligodeoxynucleotides were determined from the calculated extinction coefficients at 260 nm (*34*). The two strands were mixed at an ∼1:1 molar ratio. The mixtures were heated to 75 °C for the modified and 85 °C for the unmodified DNA for 5 min before being cooled to room temperature. The annealed duplexes were eluted from hydroxylapatite. Samples for NMR were prepared with a buffer solution of 0.1 M NaCl, 10 mM NaH_2PO_4, and 50 μM Na_2EDTA (pH 6.8). To examine nonexchangeable protons, sample solutions were lyophilized and exchanged with 99.96% D_2O three times. The final solution was reconcentrated with 99.996% D_2O to a strand concentration of 1.2 mM in 0.25 mL in a micro tube (Shigemi, Inc.) for the N^2-(3-oxo-1-propenyl)-dG-modified oligodeoxynucleotide and 2.0 mM in 0.5 mL in a 5 mm tube for the unmodified sample. Samples that were used for examining exchangeable protons were prepared in the above buffer solution containing 9:1 H_2O/D_2O.

UV Melting Experiments. The melting experiments were carried out in a Varian Cary 4E spectrophotometer. The studies were performed in the buffer with 10 mM sodium phosphate, 0.05 mM Na_2EDTA, and 1 M NaCl (pH 7.0). This solution was degassed. The temperature was increased at a rate of 0.5 °C/min from 2 to 90 °C. Ultraviolet absorbance was measured at 260 nm. The melting temper-

[1] Abbreviations: EDTA, ethylenediaminetetraacetic acid; HPLC, high-pressure liquid chromatography; NMR, nuclear magnetic resonance; NOE, nuclear Overhauser enhancement; M_1G, 3-(β-D-ribofuranosyl)pyrimido[1,2-*a*]purin-10(3*H*)-one; MDA, malondialdehyde; PdG, 1,N^2-propano-2′-deoxyguanosine; DMT, dimethoxytrityl; DSS, 2,2-dimethyl-2-silapentane-5-sulfonate; ring-opened M_1G, N^2-(3-oxo-1-propenyl)-dG; TPPI, time-proportional phase increment; TOCSY, total homonuclear correlated spectroscopy. The oligodeoxynucleotides discussed in this paper do not have terminal phosphate groups; we abbreviate the nomenclature for oligodeoxynucleotides by leaving out the phosphodiester linkage. A, C, G, T, and X refer to mononucleotide units; X is the ring-opened M_1G, N^2-(3-oxo-1-propenyl)-dG. A right superscript refers to numerical position in the oligodeoxynucleotide sequence starting from the 5′-terminus of chain A and proceeding to the 3′-terminus of chain A and then from the 5′-terminus of chain B to the 3′-terminus of chain B. To keep the numbering scheme in register with previous studies with d(CGCXCGGCATG)·d(CATGCCGCGCG), the nucleotides have been numbered beginning with A^{-2}, T^{-1}, C^{1}, etc. C2, C5, C6, C8, C1′, C2′, C2″, etc., represent specific carbon nuclei. H2, H5, H6, H8, H1′, H2′, H2″, etc., represent the protons attached to these carbons. Note the change in the numbering scheme for M_1G, where the imidazole proton of the purine ring is labeled H2.

ature T_m was determined as the midpoint of the double strand−single strand transition.

NMR Experiments. NOESY and DQF-COSY experiments were performed at a ^{1}H frequencies of 750.13 or 500.13 MHz. DSS was used as a reference for the spectra. Phase-sensitive NOESY spectra used for resonance assignment were recorded using TPPI phase cycling with a mixing time of 300 ms. For examination of exchangeable protons, phase-sensitive NOESY experiments were carried out in 9:1 H_2O/D_2O using a field-gradient Watergate pulse sequence (*35*) for water suppression. The spectra were recorded at 10 °C with a mixing time of 250 ms. Phase-sensitive TOCSY spectra were obtained using a 105 ms MLEV17 (*36*) spin lock pulse at 2 G for mixing with TPPI quadrature detection. The data were generally recorded with 1024 real data points in the d_1 dimension and 2048 real data points in the d_2 dimension. To derive distance restraints, NOESY spectra were recorded at mixing times of 150, 250, and 350 ms. The NOESY pulse program was modified to eliminate artifacts arising from zero-quantum coherence and zz terms observed at short mixing times. A systematically shifted composite 180° pulse was implemented within the mixing period, and composite 90° pulses were used in place of the second and third 90° pulses in the standard pulse sequence (*37*). The data were processed using FELIX (Molecular Simulations, Inc., San Diego, CA) on an Indigo^2 workstation (Silicon Graphics, Inc., Mountain View, CA). The data in the d_1 dimension were zero-filled to give a matrix of 2048 × 2048 real points. A skewed sine-bell square apodization function with a 90° phase shift was used in both dimensions.

Structure Refinement. Classical B-DNA and A-DNA (*38*) were used as the reference structures to create starting structures for the refinement. The initial model of the N^2-(3-oxo-1-propenyl)-dG-adducted oligomer was constructed using the BUILDER module of INSIGHTII (Molecular Simulations, Inc.). The atomic charges of N^2-(3-oxo-1-propenyl)-dG were assigned using the calculated results from MOPAC (*39*), and are listed in Table 1S of the Supporting Information. The two reference structures were energy minimized for 500 iterations by the conjugate gradient method to give the starting structures, N^2-(3-oxo-1-propenyl)-dG-Bi and N^2-(3-oxo-1-propenyl)-dG-Ai, respectively. Stereoviews of these are shown in Figure 1S of the Supporting Information. Footprints were drawn around the NOE cross-peaks for the NOESY spectrum measured with a mixing time of 350 ms to define the size and shape of the individual cross-peak using FELIX. The same set of footprints was applied to spectra measured with other mixing times. Cross-peak intensities were determined by volume integration of the areas under the footprints. The intensities were combined as necessary with intensities generated from complete relaxation matrix analysis of a starting DNA structure to generate a hybrid intensity matrix. MARDIGRAS (*40*) was used to iteratively refine the hybrid matrix to optimize the agreement with experimental NOE intensities. Calculations using DNA starting models generated by INSIGHTII, NOE experiments with three mixing times, and a DNA correlation time of 2, 3, and 4 ns yielded nine sets of distances. These data were pooled; average values of all minimum and maximum distances were used in setting error bounds to give the experimental NOE restraints used in subsequent molecular dynamics calculations (*32*).

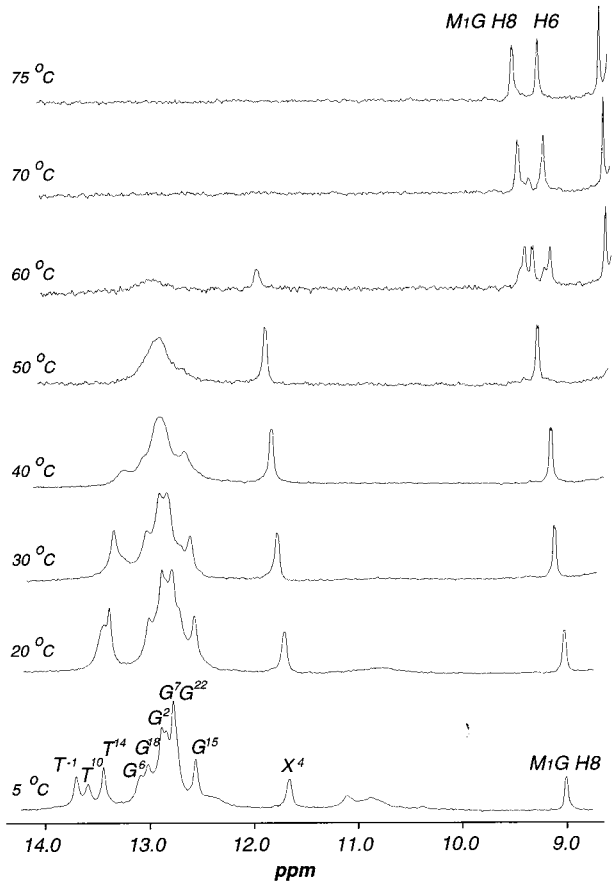

FIGURE 1: Expanded imino proton region of the N^2-(3-oxo-1-propenyl)-dG-modified *hisD3052* oligonucleotide duplex. ^{1}H spectra are shown as a function of temperature. The N^2-(3-oxo-1-propenyl)-dG derivative shows the imino resonance of X^4 N1H at 11.6 ppm and the H8 proton of the N^2-(3-oxo-1-propenyl)-dG derivative at 9 ppm; above the T_m, the N^2-(3-oxo-1-propenyl)-dG derivative recyclizes to M_1G, with the M_1G H6 and H8 signals observed at ∼9 ppm. At 60 °C, resonances for both the N^2-(3-oxo-1-propenyl)-dG derivative and M_1G are observed.

Molecular Dynamics and Simulated Annealing. All potential energy minimization and restrained MD calculations were performed using X-PLOR (version 2.4) (*41*) implemented with the CHARMM (*42*) force field. The empirical energy function (*43*) consisted of energy terms for bonds, bond angles, torsion angles, tetrahedral and planar geometry, hydrogen bonding, and nonbonding interactions, including van der Waals and electrostatic forces. The van der Waals energy term was approximated using the Lennard-Jones potential energy function. The electrostatic term used the Coulomb function, based on a full set of partial charges (−1 per residue). A distance-dependent dielectric constant of 4 was applied for all calculations. The nonbonding pair list was updated if any atom moved more than 0.5 Å, and a cutoff distance of 11 Å was used for the nonbonding interactions. The effective energy function was composed of two terms describing distance and dihedral restraints, which were in the form of a square well potential (*44*). All bond lengths involving hydrogen were kept fixed with the SHAKE algorithm (*45*) during MD calculations. The integration time step used in the molecular dynamics calculations was 1 fs. Structure coordinates were archived every 0.1 ps. All calculations were performed in vacuo without explicit counterions. The final refined structure was obtained by minimizing the averaged structure generated from 12 struc-

Table 1: Chemical Shifts of Exocyclic Protons of the N^2-(3-Oxo-1-propenyl)-dG Lesion

proton	single-stranded M_1G oligomer[a] (ppm)	single-stranded N^2-(3-oxo-1-propenyl)-dG oligomer[b] (ppm)	double-stranded N^2-(3-oxo-1-propenyl)-dG oligomer (ppm)	$\Delta\delta_1$[c] ($\delta_{ss-M_1G} - \delta_{ds}$)	$\Delta\delta_2$[d] ($\delta_{ss-M_1G} - \delta_{ds}$)
H2	8.48	7.58	7.98	−0.40	0.50
H6	8.76	7.82	7.79	0.03	−0.15
H7	7.56	5.68	5.78	−0.10	1.78
H8	9.45	9.01	8.95	0.06	0.50

[a] Measured under the same conditions before the sample was annealed with the complementary strand. [b] From ref *28*. [c] Chemical shift change $\Delta\delta = \delta_{ring-opened-form-in-single-strand} - \delta_{ring-opened-form-in-duplex}$. Values for the ring-opened form in the single strand were measured at pH 10 without calibrating the pH effect. [d] Chemical shift change $\Delta\delta = \delta_{ring-closed-form-in-single-strand} - \delta_{ring-opened-form-in-duplex}$.

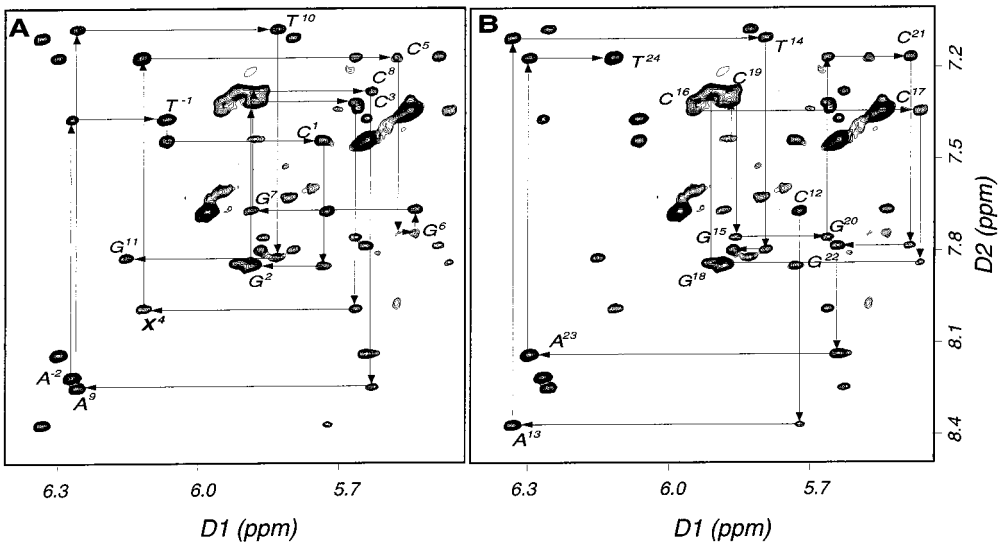

FIGURE 2: Expanded plots from the aromatic−anomeric region of the 750.13 MHz NOESY spectrum with a mixing time of 350 ms, showing sequential connectivities of the N^2-(3-oxo-1-propenyl)-dG-modified *hisD3052* oligonucleotide: (A) the modified strand and (B) the complementary strand.

tures from two MD calculations, six from an A-form starting structure, iniA, and six from a B-form starting structure, iniB. Further details of the rMD calaculations are provided in the Supporting Information. Back-calculation of NMR data was performed using CORMA (*46*) on the final refined structure excluding two terminal base pairs.

RESULTS

Formation and Thermal Stability of Ring-Opened M_1G. The introduction of M_1G into the *hisD3052* oligodeoxynucleotide duplex resulted in the spontaneous and quantitative opening of the 1,N^2-exocyclic ring of M_1G to N^2-(3-oxo-1-propenyl)-dG. Figure 1 shows the imino proton region of a series of one-dimensional ^{1}H NMR spectra recorded as a function of temperature. At temperatures below 60 °C, conditions under which the oligodeoxynucleotide sample existed as duplex DNA, the guanine imino N1H resonance of N^2-(3-oxo-1-propenyl)-dG was observed at 11.6 ppm. Integration indicated 11 imino protons; the imino protons of the terminal base pairs were not observed due to resonance broadening due to exchange with solvent. The resonance at 9.0 ppm at 30 °C was attributed to the H8 proton of N^2-(3-oxo-1-propenyl)-dG. Below the melting temperature, this resonance shifted downfield as the temperature increased. When the duplex melted at higher temperatures, the imino protons underwent rapid exchange with solvent and disappeared from the spectrum. The complete dissociation of the duplex above 75 °C resulted in recyclization which formed M_1G, evidenced by the H8 resonance observed at 9.5 ppm and the H6 resonance observed at 8.9 ppm. A slow cooling of the completely heat-denatured sample from 85 °C to room temperature reproduced the spectrum of N^2-(3-oxo-1-propenyl)-dG.

The presence of ring-opened M_1G in the duplex DNA was further confirmed by analysis of chemical shifts and scalar couplings of the exocyclic protons, i.e., H6−H8, of N^2-(3-oxo-1-propenyl)-dG. In the N^2-(3-oxo-1-propenyl)-dG-modified duplex, the H6−H8 resonances were observed at 7.9, 5.7, and 8.0 ppm, respectively, consistent with N^2-(3-oxo-1-propenyl)-dG, and not M_1G (Table 1). The M_1G imidazole H2 proton shifted from 8.4 to 8.0 ppm, also consistent with N^2-(3-oxo-1-propenyl)-dG. In addition, the scalar couplings of H6−H8 resonances corresponded to the ring-opened species. A coupling constant $J_{H7,H8}$ of 12 Hz was recorded, indicative of coupling from an aldehyde proton to a trans vinylic system. Likewise, a $J_{H6,H7}$ of 18 Hz was consistent with a trans orientation about the vinylic bond. The long-range coupling $J_{H6,H8}$ was concluded to be <5 Hz since it was not resolved. The trans configuration was further evidenced by observing a stronger NOE between H6 and H8 than between H7 and H6, or between H7 and H8. The increased line widths of the H6−H8 proton resonances were attributed to the equilibrium between the ring-opened N^2-(3-oxo-1-propenyl)deoxyguanosine and the corresponding enol. Also, the exchangeable NH proton in the aldehyde tautomer broadened the H6 resonance.

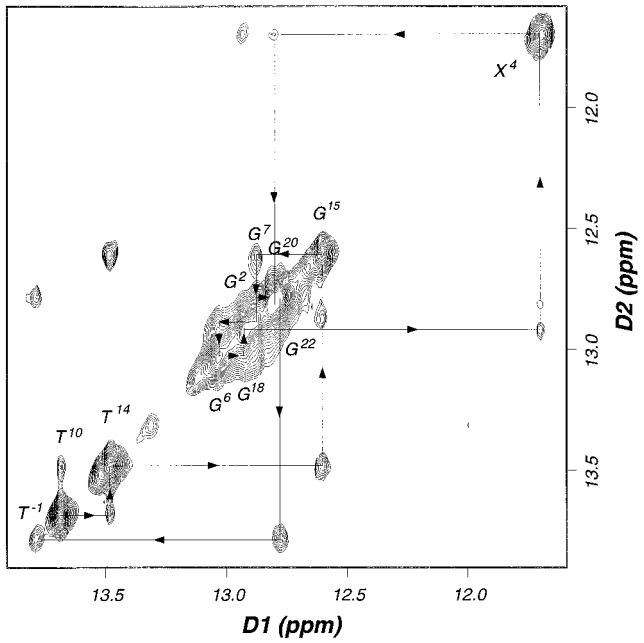

FIGURE 3: Expanded plot showing the sequential NOE connectivities for the imino protons of the N^2-(3-oxo-1-propenyl)-dG-modified *hisD3052* oligonucleotide duplex. The imino proton of the N^2-(3-oxo-1-propenyl)-dG derivative shows sequential connectivities to its neighbors G^{18} and G^{20}.

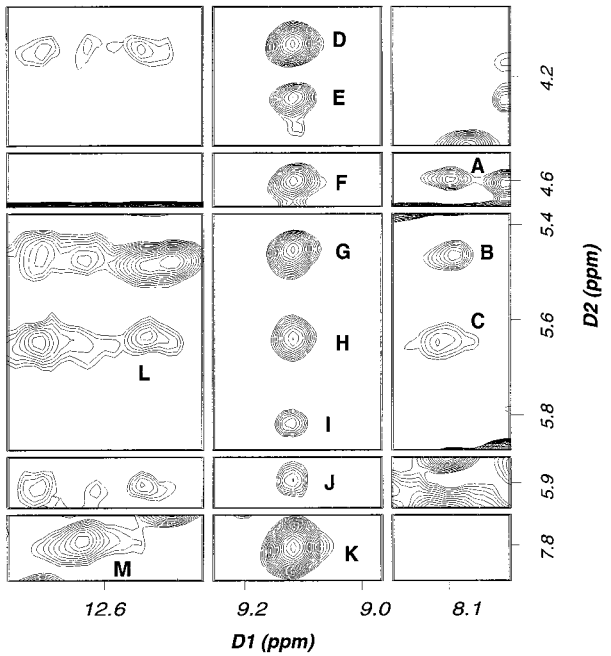

FIGURE 4: Tile plots showing selected NOE cross-peaks between 3-oxo-1-propenyl protons of N^2-(3-oxo-1-propenyl)-dG and DNA protons: (A) X^4 H6 → G^{20} H4′, (B) X^4 H6 → G^{20} H1′, (C) X^4 H6 → X^4 H7, (D) X^4 H8 → G^{20} H5′, (E) X^4 H8 → G^{20} H5″, (F) X^4 H8 → G^{20} H4′, (G) X^4 H8 → G^{20} H1′, (H) X^4 H8 → X^4 H7, (I) X^4 H8 → C^{19} H1′, (J) X^4 H8 → C^{18} H1′, (K) X^4 H8 → X^4 H6, (L) X^4 H7 → G^{20} N1H, and (M) X^4 H6 → G^{18} N1H.

The presence of the N^2-(3-oxo-1-propenyl)-dG lesion decreased the thermal stability of the *hisD3052* oligodeoxynucleotide duplex. Melting temperatures for the native and N^2-(3-oxo-1-propenyl)-dG-modified oligodeoxynucleotides were 73 and 59 °C, respectively, as determined by UV absorbance. This was compared to that of the corresponding PdG-modified *hisD3052* oligodeoxynucleotide, which exhibited a T_m of 48 °C under comparable conditions. Thus, the N^2-(3-oxo-1-propenyl)-dG-adducted duplex was destabilized relative to the unmodified duplex, but was more stable than the PdG-modified duplex. Thermal melting studies showed that the thermal denaturation of the N^2-(3-oxo-1-propenyl)-dG-modified oligodeoxynucleotide duplex was independent of pH in the range of 5−7.

Assignments of Nonexchangeable DNA Protons. The sequential assignments for both the unmodified and modified *hisD3052* oligodeoxynucleotide were accomplished using standard protocols (*47*, *48*) by analyzing NOESY, DQF-COSY, and TOCSY spectra. Parallel experiments for the unmodified *hisD3052* oligonucleotide duplex revealed that the NOE connectivities of nonexchangeable and exchangeable protons of the unmodified sample exhibited the features of B-like DNA. For the N^2-(3-oxo-1-propenyl)-dG-modified *hisD3052* oligonucleotide, complete sets of aromatic proton to anomeric proton sequential connectivities were observed (Figure 2) for both modified and complementary strands. There were no interruptions to the sequential NOEs at or adjacent to the adducted site. This confirmed that the N^2-(3-oxo-1-propenyl)-dG lesion remained stacked into the intact duplex. However, the connectivity C^5 H1′ → G^6 H8 was weak. Likewise, the connectivity between neighboring base aromatic protons C^5 H6 → G^6 H8 was absent. The complete assignments of nonexchangeable protons of unmodified and N^2-(3-oxo-1-propenyl)-dG-modified *hisD3052* oligonucleotide are summarized in Tables 2S and 3S of the Supporting Information.

Assignments of Exchangeable DNA Protons. The expanded imino proton region from a ^{1}H NOESY experiment (Figure 3) showed the sequential NOE connectivity observed between the imino protons of the N^2-(3-oxo-1-propenyl)-dG-modified *hisD3052* duplex. Compared with those of the native oligodeoxynucleotide, the imino protons exhibited small changes in chemical shifts. The NOEs between imino N1H of the N^2-(3-oxo-1-propenyl)-dG nucleotide X^4 (11.6 ppm) and adjacent G^{18} N1H and G^{20} N1H were weaker than the remainder of the imino-to-imino cross-peaks. The upfield shift of X^4 N1H suggested that the imino proton of N^2-(3-oxo-1-propenyl)-dG did not participate in Watson−Crick hydrogen bonding with C^{19}. This was supported by the absence of cross-peaks between X^4 N1H and the amino protons of C^{19}, which were observed in the ^{1}H spectrum at 6.42 ppm.

NOE Connectivities between N^2-(3-Oxo-1-propenyl)-dG and DNA. A total of nine cross-peaks were assigned between the N^2-(3-oxo-1-propenyl)-dG H6−H8 protons and nonexchangeable protons of DNA. Several of these are presented as tile plots in Figure 4. The N^2-(3-oxo-1-propenyl)-dG H8 had cross-peaks of medium intensity to C^{19} H1′, G^{20} H1′, G^{20} H4′, and G^{20} H5′ and H5″. Weak cross-peaks were observed between N^2-(3-oxo-1-propenyl)-dG H6 and H7 to C^{19} H1′ and N^2-(3-oxo-1-propenyl)-dG H6 and H7 to C^5 H1′. In addition, three NOEs were observed between N^2-(3-oxo-1-propenyl)-dG H6 and H7 and exchangeable protons of DNA. Medium-intensity cross-peaks were observed between H6 and G^{18} N1H, and H8 and C^5 N2H_a. A weak cross-peak was observed between H7 and G^{20} N1H. A NOESY experiment also revealed that weak NOEs were observed between all three N^2-(3-oxo-1-propenyl)-dG protons, H6−H8, and X^4 N1H. The observed NOEs between N^2-(3-oxo-1-propenyl)-dG and DNA protons primarily involved DNA

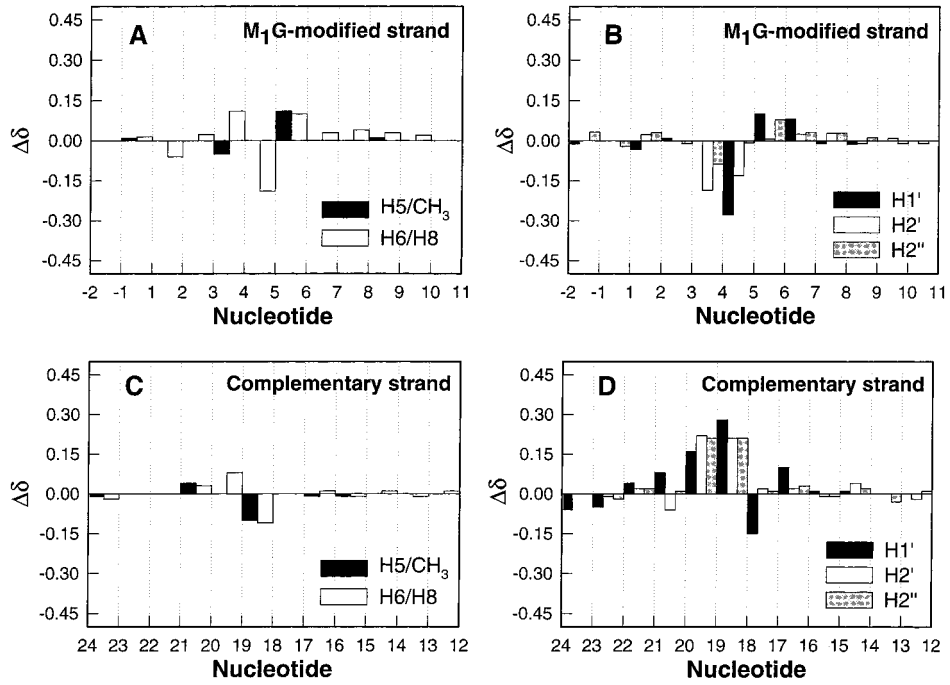

FIGURE 5: Chemical shift changes of selected protons relative to those of the unmodified oligodeoxynucleotide duplex. (A) Major groove base protons of the N^2-(3-oxo-1-propenyl)-dG-modified strand. (B) Minor groove deoxyribose protons of the N^2-(3-oxo-1-propenyl)-dG-modified strand. (C) Major groove base protons of the complementary strand. (D) Minor groove deoxyribose protons of the complementary strand. $\Delta\delta = [\delta_{\text{unmodified-oligodeoxynucleotide}} - \delta_{\text{modified-oligodeoxynucleotide}}]$ (parts per million).

protons located in the minor groove as opposed to the major groove and exchangeable protons, suggesting that the N^2-(3-oxo-1-propenyl) moiety was positioned in the minor groove.

Chemical Shift Perturbations. Figure 5 shows a comparison of the chemical shifts of selected nonexchangeable protons between the unmodified and N^2-(3-oxo-1-propenyl)-dG-modified *hisD3052* oligodeoxynucleotides. Most of the nonexchangeable protons of the N^2-(3-oxo-1-propenyl)-dG-modified oligodeoxynucleotide showed little or no chemical shift changes relative to those of the unmodified form. Protons with large chemical shift changes (>0.2 ppm) were from nucleotides near the adducted site. Relative to those of the unmodified oligomer, G^{18} H8, C^5 H5, and C^{19} H5 shifted downfield and C^5 H5 shifted upfield. C^{19} H6 and H5 shifted downfield 0.12 and 0.13 ppm, respectively. C^3 and C^5 H6 exhibited upfield chemical shifts of 0.14 and 0.13 ppm, respectively, relative to those of the unmodified form. In addition, chemical shift changes were observed in several sugar protons from the nucleotides of both modified and complementary strands; most of them were located adjacent to the N^2-(3-oxo-1-propenyl)-dG-modified site. G^{18} H1′ shifted downfield about 0.15 ppm. C^{19} H1′ and G^{20} H1′ shifted upfield 0.29 and 0.15 ppm, respectively. C^5 H1′ shifted upfield 0.10 ppm. C^5 H2″ shifted upfield 0.1 ppm. X^4 H1′ (M_1G) shifted downfield 0.26 ppm. X^4 H2″ shifted downfield 0.10 ppm as well. Interestingly, chemical shift perturbations were observed for some sugar protons of G^6 and C^{17}, which comprised the second base pair from the adduction site in the 3′-direction. C^{17} H1′ shifted upfield 0.12 ppm, and G^6 H1′ also exhibited a 0.1 ppm upfield change. Among the exchangeable protons, the non-hydrogen-bonded X^4 N1H shifted upfield 1.24 ppm; G^{18} N1H shifted downfield ~0.10 ppm, and G^{20} N1H shifted upfield about 0.1 ppm in the N^2-(3-oxo-1-propenyl)-dG-modified oligodeoxynucleotide relative to that of the unmodified oligodeoxynucleotide. There were no significant chemical shift changes for the remaining imino protons. The 3-oxopropenyl protons, H6−H8, exhibited <0.1 ppm chemical shift changes compared to those measured for the single-stranded oligonucleotide containing N^2-(3-oxo-1-propenyl)-dG. Compared with the PdG-modified *hisD3052* duplex, in which PdG was intercalated in the duplex in the syn conformation, H6−H8 of N^2-(3-oxo-1-propenyl)-dG exhibited a much smaller scale of chemical shift changes.

Structure Refinement. A total of 602 NOEs were utilized to derive the distances using MARDIGRAS. These distances, and 26 additional empirical restraints for hydrogen bonding, were applied as distance restraints in rMD calculations. The distribution of the experimental restraints is presented in Figure 6. To prepare the starting structures used for rMD calculations, the 3-oxopropenyl moiety was constructed with the trans conformation at the vinylic bond, based on the experimentally measured *J* couplings of vinyl protons as well as NOEs from these protons. The final refined structure was generated from the energy-minimized average structure from sets of rMD calculations, obtained from either an A-form starting structure or a B-form starting structure.

The precision of the structural refinement proceeding from either the B-form N^2-(3-oxo-1-propenyl)-dG-Bi or A-form N^2-(3-oxo-1-propenyl)-dG-Ai starting structure was evaluated by pairwise rms deviation of the emergent structures (Table 2). Figure 7 shows superimposed six structures from the rMD calculations. The fact that the emergent structures exhibited only minimal structural perturbation from B-DNA was evidenced by the pairwise rmsd of 0.76 Å between the N^2-(3-oxo-1-propenyl)-dG-Bi starting structure and the set of six structures which emerged from the calculations starting from N^2-(3-oxo-1-propenyl)-dG-Bi. In contrast, the pairwise rmsd between N^2-(3-oxo-1-propenyl)-dG-Ai and the set of

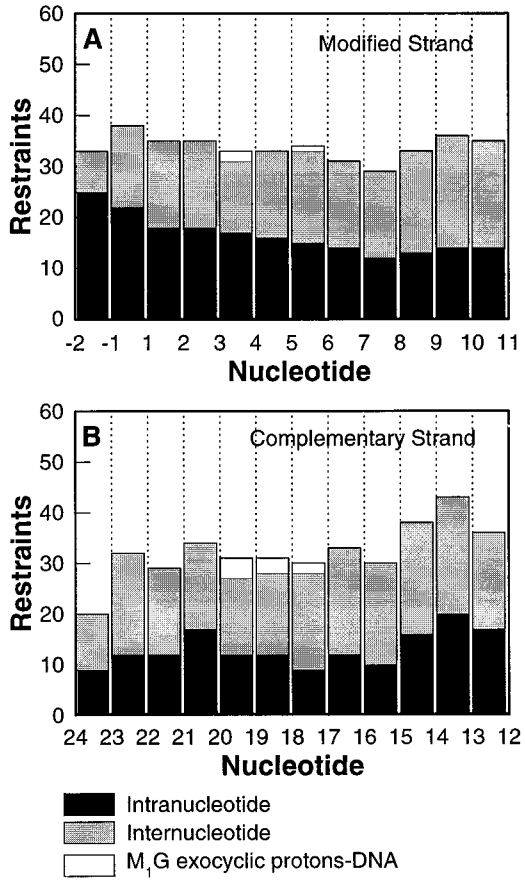

FIGURE 6: Distribution of the experimental restraints derived from NOESY data. Internucleotide NOEs are defined as those from residue i to residue $i + 1$.

six structures which emerged from the calculations starting from N^2-(3-oxo-1-propenyl)-dG-Ai was 5.6 Å, indicating that the emergent structures were not A-like.

The agreement between the calculated structures and the experimental data was evaluated by analysis of sixth-root residuals, R_1^x, listed in Table 3. The residual R_1^x value of 9.1×10^{-2} suggested that the calculated structures were in reasonable agreement with the NMR data. The final emergent structures gave R_1^x values of $8.8-8.9 \times 10^{-2}$ for intranucleotide NOEs and $9.0-9.5 \times 10^{-2}$ for internucleotide NOEs, irrespective of the starting structure. The observation that the R_1^x values for the final structures were only slightly improved over those calculated for the N^2-(3-oxo-1-propenyl)-dG-Bi starting structure provided further support for the conclusion that the minor groove N^2-(3-oxo-1-propenyl)-dG adduct resulted in only minor structural perturbation of the B-DNA duplex.

DISCUSSION

This work continues our study of 1,N^2-exocyclic deoxyguanosine lesions in the frameshift-prone iterated CG repeat sequence from the *hisD3052* gene of *S. typhimurium*. The iterated repeat contained in the *hisD3052* oligodeoxynucleotide is thought to be prone to frameshifts by slippage of either the template or the primer strand during DNA replication (*49*). The *hisD3052* mutation arose from the histidinol dehydrogenase gene of *S. typhimurium* by deletion of a cytosine induced by ICR-191 (*50*, *51*). It is reversed by additions and deletions that restore the reading frame but

Table 2: Root-Mean-Square (rms) Deviations, Excluding the Terminal Base Pairs, between the Initial Structures, the Various rMD Structures, and Final Average Structures of the N^2-(3-Oxo--1-propenyl)-dG-Modified *hisD3052* Oligodeoxynucleotide

	atomic rms difference (Å)
initial structures	
M_1G-Ai vs M_1G-Bi	8.18
rms shifts	
M_1G-Ai vs ⟨rMD M_1G-Ai⟩[a]	5.63 ± 0.42
M_1G-Bi vs ⟨rMD M_1G -Bi⟩[b]	0.76 ± 0.32
rms distributions	
⟨rMD M_1G-Ai⟩ vs ⟨rMD M_1G-Ai⟩	0.80 ± 0.10
⟨rMD M_1G-Bi⟩ vs ⟨rMD M_1G-Bi⟩	0.78 ± 0.17
⟨rMD M_1G-Ai⟩ vs ⟨rMD M_1G-Bi⟩	1.03 ± 0.29
⟨rMD M_1G-Ai⟩ vs rMD[c]	0.90 ± 0.19
⟨rMD M_1G-Bi⟩ vs rMD	0.87 ± 0.16

[a] ⟨rMD M_1G-Ai⟩ represents the set of six structures which emerged from MD calculations starting with rMD M_1G-Ai. [b] ⟨rMD M_1G-Bi⟩ represents the set of six structures which emerged from MD calculations starting from M_1G-Bi. [c] rMD represents the average minimized structure from all 12 MD calculations.

Table 3: Comparison of Sixth-Root Residual Indices R_1^x for Starting Models and the Resulting MD Structures[a−c]

	intranucleotide R_1^x	internucleotide R_1^x	overall R_1^x
M_1G-Ai	9.5	11.6	10.8
M_1G-Bi	9.1	9.4	9.3
⟨MDA⟩	8.9	9.5	9.3
⟨MDB⟩	8.8	9.0	8.9
⟨rMDav⟩	8.8	9.4	9.1

[a] Only the inner 11 base pairs were used in the calculations, to exclude end effects. The mixing time was 350 ms. [b] $R_1^x = \Sigma|(a_o)_i^{1/6} - (a_c)_i^{1/6}|/\Sigma|(a_o)_i^{1/6}|$, where a_o and a_c are the intensities of observed (nonzero) and calculated NOE cross-peaks, respectively. [c] N^2-(3-Oxo-1-propenyl)-dG-Ai, starting energy-minimized ring-opened M_1G modified A-DNA; N^2-(3-oxo-1-propenyl)-dG-Bi, starting energy-minimized N^2-(3-oxo-1-propenyl)-dG modified Bi; ⟨MDA⟩, average of six rMD structures starting from N^2-(3-oxo-1-propenyl)-dG-Ai; ⟨MDB⟩, average of six rMD structures starting from N^2-(3-oxo-1-propenyl)-dG-Bi; ⟨rMDav⟩, average of 12 rMD structures starting from N^2-(3-oxo-1-propenyl)-dG-Ai and N^2-(3-oxo-1-propenyl)-dG-Bi.

do not necessarily reverse the forward mutation (*52*). The most common reversion event is a CG deletion in the reiterated sequence $(CG)_4$ (*53*−*56*).

Our interest in the structure of N^2-(3-oxo-1-propenyl)-dG embedded into the frameshift-prone *hisD3052* iterated CG repeat sequence arose from two observations. The first was that MDA, a small alkylating agent, induced frameshift mutations (*57*) despite the fact that frameshift mutations are more commonly associated with DNA intercalators. The second was that the primary lesion induced by MDA, the 3-(2′-deoxy-β-D-*erythro*-pentofuranosyl)pyrimido[1,2-*a*]purin-10(3*H*)-one (M_1G), spontaneously converted to its N^2-(3-oxo-1-propenyl)-dG derivative when inserted into duplex DNA opposite cytosine in the complementary strand. This ring opening was reversible such that upon denaturation of the DNA duplex, M_1G was regenerated (*28*) (Figure 1).

Structure of the N^2-(3-Oxo-1-propenyl)-dG Lesion. The significant result of this work was the observation that the N^2-(3-oxo-1-propenyl)-dG lesion creates relatively little structural perturbation of the B-DNA duplex; the 3-oxo-1-propenyl moiety extends into the minor groove. Figure 8 shows the stacking orientation of the N^2-(3-oxo-1-propenyl)-dG lesion relative to its neighboring bases, and in comparison to the corresponding unmodified *hisD3052* oligodeoxynucle-

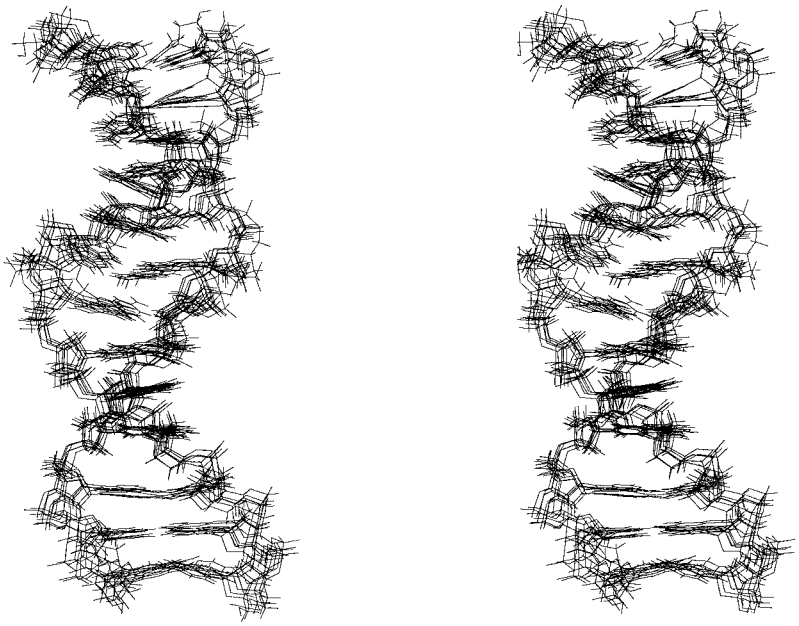

FIGURE 7: Stereoview showing six superimposed structures that emerge from the restrained MD−simulated annealing protocol, beginning from the N^2-(3-oxo-1-propenyl)-dG-Bi starting structure.

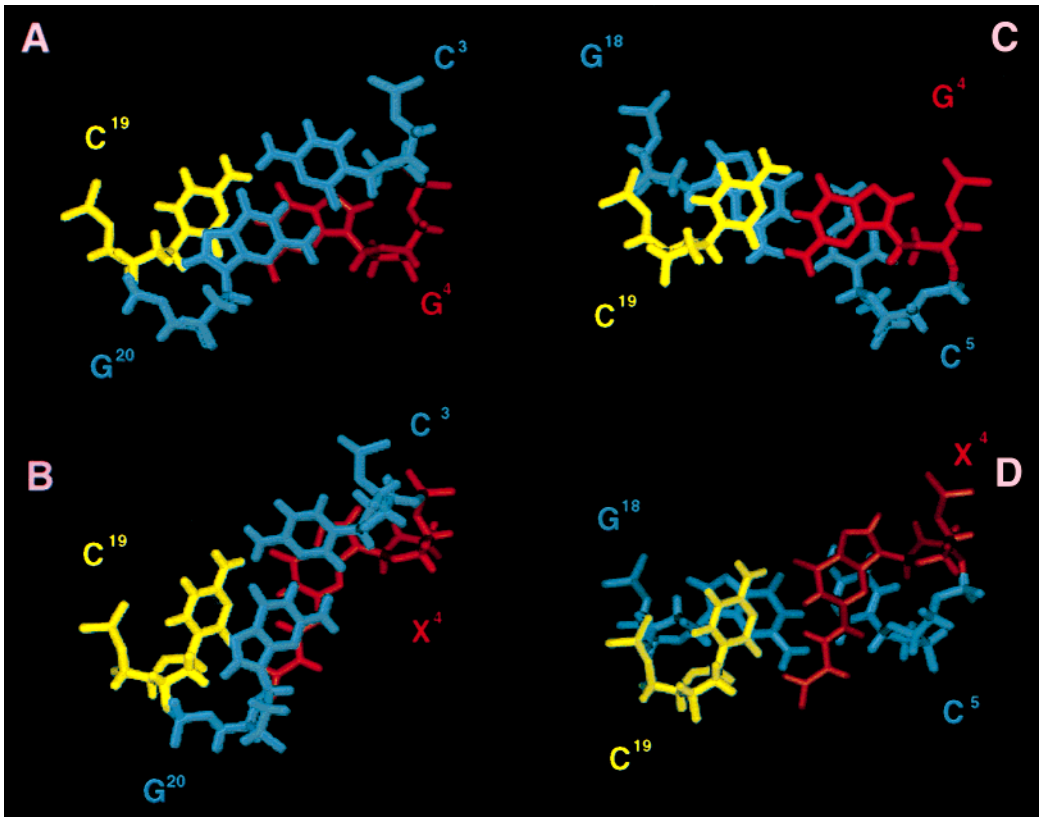

FIGURE 8: Stacking patterns of the N^2-(3-oxo-1-propenyl)-dG lesion relative to neighboring base pairs. (A) Base step $C^3 \cdot G^{20} \rightarrow G^4 \cdot C^{19}$ for the unmodified oligodeoxynucleotide. (B) Base step $G^4 \cdot C^{19} \rightarrow C^5 \cdot G^{18}$ for the unmodified oligodeoxynucleotide. (C) Base step $C^3 \cdot G^{20} \rightarrow X^4 \cdot C^{19}$ for the N^2-(3-oxo-1-propenyl)-dG-modified oligodeoxynucleotide. (D) Base step $X^4 \cdot C^{19} \rightarrow C^5 \cdot G^{18}$ for the N^2-(3-oxo-1-propenyl)-dG-modified oligodeoxynucleotide.

otide duplex. The largest structural alteration predicted by the calculations was the protrusion of the complementary cytosine, C^{19}, toward the major groove, concomitant with the loss of Watson−Crick hydrogen bonding at the adducted base pair. This predicted loss of hydrogen bonding was consistent with the NMR data which showed an upfield shift of the X^4 N1H proton, and with thermal melting data, which showed a 14 °C decrease in T_m. The displacement of C^{19} also allowed the 3-oxopropenyl moiety of N^2-(3-oxo-1-propenyl)-dG to be accommodated in the minor groove without inducing large-scale structural rearrangement.

Several lines of experimental evidence confirmed the intrahelical orientation of the modified guanine. The NOE cross-peak between N^2-(3-oxo-1-propenyl)-dG H1′ and H8 exhibited an intensity comparable to that of the unmodified nucleotide, supporting the conclusion that the N^2-(3-oxo-1-

propenyl)-dG remained in the anti conformation. Most of the observed adduct−DNA NOE connectivities arose between the 3-oxo-1-propenyl protons of the N^2-(3-oxo-1-propenyl)-dG and nonexchangeable protons of the complementary strand opposite the adduction site. The cross-peaks between N^2-(3-oxo-1-propenyl)-dG H8 and G^{20} H1′ and H4′ and weaker cross-peaks between N^2-(3-oxo-1-propenyl)-dG H8 and H6 and C^{19} H1′ positioned the 3-oxo-1-propenyl moiety of the N^2-(3-oxo-1-propenyl)-dG toward the minor groove. The neighboring base pairs C^3•G^{20} and C^5•G^{18} remained hydrogen-bonded. They were predicted to be buckled relative to the unmodified oligodeoxynucleotide. This was consistent with the experimentally observed interruption between C^5 and G^6 as well as with a relatively weak NOE between H1′ and G^6 H8 and very weak NOEs between X^4 N1H and the neighboring G^{18} and G^{20} imino protons. The chemical shift data (Figure 5) supported the conclusion that the modified dG residue remained inserted into the DNA helix. The small $\delta\Delta$ values of $\leq$0.15 ppm for the base protons suggested that the N^2-(3-oxo-1-propenyl)-dG adduct did not substantially alter ring-current shielding effects at the adduct site. Overall, base stacking was judged to be similar to that of the unmodified oligonucleotide duplex, but with the complementary base C^{19} shifted toward the major groove (Figure 8). We conclude that the N^2-(3-oxo-1-propenyl)-dG adduct induced minor perturbations to the DNA structure, which were localized near the adduct site.

Comparison of the N^2-(3-Oxo-1-propenyl)-dG Derivative with Intact M_1G. The fact that M_1G spontaneously ring opens to the N^2-(3-oxo-1-propenyl)-dG derivative in duplex DNA leaves the conformation of intact M_1G in DNA to be determined. One clue about the behavior of intact M_1G in DNA comes from examination of its structural analogue PdG. The conformation of the PdG adduct in the *hisD3052* oligomer differed considerably from the corresponding site-specific N^2-(3-oxo-1-propenyl)-dG adduct. With PdG, modification resulted in an ~24 °C decrease in T_m, and NMR revealed a complex set of pH-dependent conformational equilibria, which involved the glycosyl bonds of the modified base and its 3′-neighbor. At pH 5.8, PdG was rotated about the glycosyl bond from the anti to the syn conformation, placing the exocyclic lesion into the major groove of the DNA (*29*). The substantial conformational differences between N^2-(3-oxo-1-propenyl)-dG and PdG, when located at equivalent positions in the *hisD3052* oligomer sequence, suggest that similarly large conformational differences may also exist between M_1G and its ring-opened derivative N^2-(3-oxo-1-propenyl)-dG.

A Configurational "Mutagenic Switch". M_1G and its ring-opened derivative may exhibit significant differences in mutagenic potential. These structural observations extend the concept of a mutagenic switch, which was first introduced to describe the possibility that two *conformations* of a DNA adduct could lead to differing mutagenic outcomes (*58*). The work presented here suggests the possibility that two *configurations* of the M_1G adduct, the intact M_1G and its ring-opened derivative, could act as a mutagenic switch. Preliminary evidence supporting of this notion exists.[2] When duplex M13 phage genomes containing a single M_1G residue opposite C were constructed and transfected into *Escherichia coli*, M_1G was observed to be weakly mutagenic. In contrast, site-specific mutagenesis experiments in which M_1G was placed into a genome opposite T, conditions under which ring opening does not occur, exhibited greater mutagenicity. The mutagenic spectrum was identical in both instances. One possible interpretation is that the N^2-(3-oxo-1-propenyl)-dG derivative of M_1G is only weakly mutagenic, and intact M_1G is the mutagenically significant species. This is consistent with the present observations that N^2-(3-oxo-1-propenyl)-dG does not induce a large structural perturbation in the DNA duplex.

To the extent that M_1G and its N^2-(3-oxo-1-propenyl)-dG derivative exhibit different susceptibilities toward mutagenesis and repair, the mutational spectrum induced by MDA is anticipated to be dependent on the relative amounts of M_1G and N^2-(3-oxo-1-propenyl)-dG present at the replication fork of the primer−template complex. Once the ring-opened N^2-(3-oxo-1-propenyl)-dG derivative is formed in duplex DNA, spontaneous ring closure is predicted to be slow. The N^2-(3-oxo-1-propenyl)-dG derivative exists with the trans conformation of the propenyl moiety, which must rearrange to the cis conformation before ring closure can occur. Future studies will focus on the rate of interconversion between M_1G and N^2-(3-oxo-1-propenyl)-dG.

MDA and Frameshift Mutagenesis. The observation that frameshifts in iterated repeats which likely occur by transient strand slippage (*49*) are more frequent with natural (*59*, *60*) and mutator polymerases (*61*−*63*) having lower processivity has led to the proposal that strand slippage may be facilitated during transient dissociation of the polymerase from DNA. Our observation that the 3-oxo-1-propenyl moiety of the N^2-(3-oxo-1-propenyl)-dG derivative is oriented into the minor groove of the *hisD3052* oligomer, where it may interfere with critical minor groove protein−DNA interactions during replication, suggests a potential role for the N^2-(3-oxo-1-propenyl)-dG derivative in frameshift mutagenesis. With polymerase β, crystallographic studies suggested Arg^{283} maintained replication fidelity, possibly by minor groove hydrogen bonding interactions with N3 (purines) or O^2 (pyrimidines) of the templating base (*64*). Replacement of Arg^{283} with Ala resulted in a reduced level of fidelity and an increased tendency toward G•A mispairing (*65*). A molecular dynamics study suggested that polymerase blockage induced by benzo[*a*]pyrene might be a consequence of disruption of hydrogen bonding between the adducted template and Arg^{283} (*66*). Alternatively, previous studies of the PdG structural analogue revealed the capability of the 1,N^2-exocyclic lesion to disrupt the modified base pair and its 3′-neighbor, representing one CG repeat unit in the iterative repeat (*29*). It will now be of interest to examine the structure of M_1G and its N^2-(3-oxo-1-propenyl)-dG derivative in the 2-BD derivative of the *hisD3052* iterated CG repeat, which models the intermediate structure leading to a two-base deletion, and in which the PdG structural analogue was examined (*30*, *31*).

The rearrangement of M_1G into its N^2-(3-oxo-1-propenyl)-dG derivative in duplex DNA suggests the potential for the latter to undergo further chemistry. One possibility is the formation of MDA-mediated interstrand cross-links, via Schiff base formation involving M_1G and DNA exocyclic amino groups. The observation that MDA mutagenesis in vivo apparently requires an intact and functioning nucleotide

[2] L. J. Marnett and co-workers, manuscript in preparation.

excision repair system (*27*, *67*) suggests that the cross-link hypothesis should be evaluated. The existence of such cross-links was inferred from biological data and chemical model studies (*68*) but has not been demonstrated in MDA-modified DNA. It will thus be of considerable interest to determine whether cytosine-catalyzed ring opening of M_1G leads to the formation of similar cross-linked species in DNA.

In summary, the solution structure of the N^2-(3-oxo-1-propenyl)-dG-modified *hisD3052* oligodeoxynucleotide exhibited minimal structural perturbations with respect to duplex DNA. Watson−Crick hydrogen bonding was not observed between the N^2-(3-oxo-1-propenyl)-dG and the complementary cytosine. The N^2-(3-oxo-1-propenyl)-dG lesion was positioned in the helix and maintained stacking interactions with the neighboring bases. The complementary cytosine was displaced, which allowed the propenyl moiety to be accommodated in the minor groove.

ACKNOWLEDGMENT

We thank Mr. Markus Voehler for assistance with collection of NMR data and Ms. Mary Kerske for assistance with preparation of the manuscript.

SUPPORTING INFORMATION AVAILABLE

A detailed description of the restrained molecular dynamics, Tables 1S−4S which list in detail partial charges calculated for the N^2-(3-oxo-1-propenyl)-dG adduct and the ^{1}H NMR assignments of the N^2-(3-oxo-1-propenyl)-dG-modified and unmodified duplexes, respectively, and Figure 1S showing stereoviews of the starting structures used in the MD refinements. This material is available free of charge via the Internet at http://pubs.acs.org.

REFERENCES

1. Pryor, W. A., and Stanley, J. P. (1975) *J. Org. Chem. 40*, 3615−3617.
2. Hamberg, M., and Samuelsson, B. (1967) *J. Biol. Chem. 242*, 5336−5343.
3. Diczfalusy, U., Falardeau, P., and Hammarstrom, S. (1977) *FEBS Lett. 84*, 271−274.
4. Mukai, F. H., and Goldstein, B. D. (1976) *Science 191*, 868−869.
5. Benamira, M., Johnson, K., Chaudhary, A., Bruner, K., Tibbetts, C., and Marnett, L. J. (1995) *Carcinogenesis 16*, 93−99.
6. Yau, T. M. (1979) *Mech. Ageing Dev. 11*, 137−144.
7. Spalding, J. W. (1988) *Natl. Toxicol. Program Tech. Rep. Ser. 331*, 5−13.
8. Marnett, L. J., Basu, A. K., O'Hara, S. M., Weller, P. E., Rahman, A. F. M. M., and Oliver, J. P. (1986) *J. Am. Chem. Soc. 108*, 1348−1350.
9. Basu, A. K., O'Hara, S. M., Valladier, P., Stone, K., Mols, O., and Marnett, L. J. (1988) *Chem. Res. Toxicol. 1*, 53−59.
10. Stone, K., Uzieblo, A., and Marnett, L. J. (1990) *Chem. Res. Toxicol. 3*, 467−472.
11. Stone, K., Ksebati, M. B., and Marnett, L. J. (1990) *Chem. Res. Toxicol. 3*, 33−38.
12. Chaudhary, A. K., Nokubo, M., Oglesby, T. D., Marnett, L. J., and Blair, I. A. (1995) *J. Mass Spectrom. 30*, 1157−1166.
13. Chaudhary, A. K., Reddy, R. G., Blair, I. A., and Marnett, L. J. (1996) *Carcinogenesis 17*, 1167−1170.
14. Seto, H., Okuda, T., Takesue, T., and Ikemura, T. (1983) *Bull. Chem. Soc. Jpn. 56*, 1799−1802.
15. Seto, H., Seto, T., Takesue, T., and Ikemura, T. (1986) *Chem. Pharm. Bull. 34*, 5079−5085.
16. Reddy, G. R., and Marnett, L. J. (1996) *Chem. Res. Toxicol. 9*, 12−15.
17. Wang, M. Y., and Liehr, J. G. (1995) *Carcinogenesis 16*, 1941−1945.
18. Chaudhary, A. K., Nokubo, M., Reddy, G. R., Yeola, S. N., Morrow, J. D., Blair, I. A., and Marnett, L. J. (1994) *Science 265*, 1580−1582.
19. Wang, M., Dhingra, K., Hittleman, W. N., Liehr, J. G., de Andrade, M., and Li, D. (1996) *Cancer Epidemiol. 5*, 705−710.
20. Nath, R. G., and Chung, F.-L. (1994) *Proc. Natl. Acad. Sci. U.S.A. 91*, 7491−7495.
21. Nath, R. G., and Chung, F. L. (1993) *Proc. Am. Assoc. Cancer Res. 34*, 137.
22. O'Nair, J., Barbin, A., Guichard, Y., and Bartsch, H. (1995) *Carcinogenesis 16*, 613−617.
23. Rouzer, C. A., Chaudhary, A. K., Nokubo, M., Ferguson, D. M., Reddy, G. R., Blair, I. A., and Marnett, L. J. (1997) *Chem. Res. Toxicol. 10*, 181−188.
24. Vaca, C. E., Fang, J. L., Mutanen, M., and Valsta, L. (1995) *Carcinogenesis 16*, 1847−1851.
25. Fang, J. L., Vaca, C. E., Valsta, L. M., and Mutanen, M. (1996) *Carcinogenesis 17*, 1035−1040.
26. Sevilla, C. L., Mahle, N. H., Eliezer, N., Uzieblo, A., O'Hara, S. M., Nokubo, M., Miller, R., Rouzer, C. A., and Marnett, L. J. (1997) *Chem. Res. Toxicol. 10*, 172−180.
27. Fink, S. P., Reddy, G. R., and Marnett, L. J. (1997) *Proc. Natl. Acad. Sci. U.S.A. 94*, 8652−8657.
28. Mao, H., Schnetz-Boutaud, N. C., Weisenseel, J. P., Marnett, L. J., and Stone, M. P. (1999) *Proc. Natl. Acad. Sci. U.S.A. 96*, 6615−6620.
29. Singh, U. S., Moe, J. G., Reddy, G. R., Weisenseel, J. P., Marnett, L. J., and Stone, M. P. (1993) *Chem. Res. Toxicol. 6*, 825−836.
30. Moe, J. G., Reddy, G. R., Marnett, L. J., and Stone, M. P. (1994) *Chem. Res. Toxicol. 7*, 319−328.
31. Weisenseel, J. P., Moe, J. G., Reddy, G. R., Marnett, L. J., and Stone, M. P. (1995) *Biochemistry 34*, 50−64.
32. Schmitz, U., and James, T. L. (1995) *Methods Enzymol. 261*, 3−44.
33. Reddy, G. R., and Marnett, L. J. (1995) *J. Am. Chem. Soc. 117*, 5007−5008.
34. Borer, P. N. (1975) in *Handbook of biochemistry and molecular biology*, CRC Press, Cleveland, OH.
35. Piotto, M., Saudek, V., and Sklenar, V. (1992) *J. Mol. Biol. 6*, 661−665.
36. Bax, A., and Davis, D. G. (1985) *J. Magn. Reson. 65*, 355−360.
37. Bodenhausen, G., Kogler, H., and Ernst, R. R. (1984) *J. Magn. Reson. 58*, 370−388.
38. Arnott, S., and Hukins, D. W. L. (1972) *Biochem. Biophys. Res. Commun. 47*, 1504−1509.
39. Hingerty, B. E., Figueroa, S., Hayden, T. L., and Broyde, S. (1989) *Biopolymers 28*, 1195−1222.
40. Borgias, B. A., and James, T. L. (1990) *J. Magn. Reson. 87*, 475−487.
41. Brunger, A. T. (1992) in *X-Plor. Version 3.1. A system for X-ray Crystallography and NMR*, Yale University Press, New Haven, CT.
42. Brooks, B. R., Bruccoleri, R. E., Olafson, B. D., States, D. J., Swaminathan, S., and Karplus, M. (1983) *J. Comput. Chem. 4*, 187−217.
43. Nilsson, L., Clore, G. M., Gronenborn, A. M., Brunger, A. T., and Karplus, M. (1986) *J. Mol. Biol. 188*, 455−475.
44. Clore, G. M., Gronenborn, A. M., Carlson, G., and Meyer, E. F. (1986) *J. Mol. Biol. 190*, 259−267.
45. Ryckaert, J.-P., Ciccotti, G., and Berendsen, H. J. C. (1977) *J. Comput. Phys. 23*, 327−341.
46. Keepers, J. W., and James, T. L. (1984) *J. Magn. Reson. 57*, 404−426.
47. Reid, B. R. (1987) *Q. Rev. Biophys. 20*, 2−28.
48. Patel, D. J., Shapiro, L., and Hare, D. (1987) *Q. Rev. Biophys. 20*, 35−112.

49. Streisinger, G., Okada, Y., Enrich, J., Newton, J., Tsugita, A., Terzaghi, E., and Inouye, M. (1966) *Cold Spring Harbor Symp. Quant. Biol. 31*, 77−84.
50. Oeschger, N. S., and Hartman, P. E. (1970) *J. Bacteriol. 101*, 490−504.
51. Hartman, P. E., Ames, B. N., Roth, J. R., Barnes, W. M., and Levin, D. E. (1986) *Environ. Mutagen. 8*, 631−641.
52. McCann, J., Spingarn, N. E., Koburi, J., and Ames, B. N. (1975) *Proc. Natl. Acad. Sci. U.S.A. 72*, 979−983.
53. Isono, K., and Yourno, J. (1974) *Proc. Natl. Acad. Sci. U.S.A. 71*, 1612−1617.
54. Fuscoe, J. C., Wu, R., Shen, N. H., Healy, S. K., and Felton, J. S. (1988) *Mutat. Res. 201*, 241−251.
55. Bell, D. A., Levine, J. G., and DeMarini, D. M. (1991) *Mutat. Res. 252*, 35−44.
56. DeMarini, D. M., Abu-Shakra, A., Gupta, R., Hendee, L. J., and Levine, J. G. (1992) *Environ. Mol. Mutagen. 20*, 12−18.
57. O'Hara, S. M., and Marnett, L. J. (1991) *Mutat. Res. 247*, 45−56.
58. Eckel, L. M., and Krugh, T. R. (1994) *Nat. Struct. Biol. 1*, 89−94.
59. Kunkel, T. A. (1985) *J. Biol. Chem. 260*, 5787−5796.
60. Kunkel, T. A. (1986) *J. Biol. Chem. 261*, 13581−13587.
61. Bebenek, K., Beard, W. A., Casas-Finet, J. R., Kim, H. R., Darden, T. A., Wilson, S. H., and Kunkel, T. A. (1995) *J. Biol. Chem. 270*, 19516−19523.
62. Minnick, D. T., Astatke, M., Joyce, C. M., and Kunkel, T. A. (1996) *J. Biol. Chem. 271*, 24954−24961.
63. Bell, J. B., Eckert, K. A., Joyce, C. M., and Kunkel, T. A. (1997) *J. Biol. Chem. 272*, 7345−7351.
64. Beard, W. A., Osheroff, W. P., Prasad, R., Sawaya, M. R., Jaju, M., Wood, T. G., Kraut, J., Kunkel, T. A., and Wilson, S. H. (1996) *J. Biol. Chem. 271*, 12141−12144.
65. Werneburg, B. G., Ahn, J., Zhong, X., Hondal, R. J., Kraynov, V. S., and Tsai, M. D. (1996) *Biochemistry 35*, 7041−7050.
66. Singh, S. B., Beard, W. A., Hingerty, B. E., Wilson, S. H., and Broyde, S. (1998) *Biochemistry 37*, 878−884.
67. Niedernhofer, L. J. (1996) Ph.D. Dissertation, Vanderbilt University, Nashville, TN.
68. Niedernhofer, L. J., Riley, M., Schnetz-Boutand, N., Sanduwaran, G., Chaudhary, A. K., Reddy, G. R., and Marnett, L. J. (1997) *Chem. Res. Toxicol. 10*, 556−561.

BI9910124